RELICT AEOLIAN BEDFORMS AND A NEW TYPE OF WIND STREAK IN THE ESA EXOMARS 2016 LANDING ELLIPSE IN MERIDIANI PLANUM, MARS. S. Silvestro[1], D. A. Vaz[2,3], G. Di Achille[4], C. Popa[1], F. Esposito[1], [1]INAF Osservatorio Astronomico di Capodimonte, Napoli, Ialy (silvestro@na.astro.it), [2]Center for Geophysics, University of Coimbra, Portugal, [3]CERENA, Lisboa, Portugal, [4]INAF, Osservatorio Astronomico di Teramo, Teramo, Italy

Introduction: The ESA 2016 ExoMars mission includes an Entry Descent and Landing Demonstrator Module (EDM) that will land on Meridiani Planum. DREAMS (Dust characterization, Risk assessment and Environment Analyzer on the Martian Surface) [1] is a meteorological station and will be onboard the EDM. Here, we present the results of an eolian characterization of the Exomars 2016 landing ellipse located between 5°W –7°W, 0° – 3°S in Terra Meridiani. The study area presents abundant aeolian features like TARs, plain ripples and wind streaks [2,3,4]. In this work we show that TARs and plains ripples present a complex spatial arrangement and we address such complexity by distinguishing different populations using geomorphic and statistic criteria. In addition, we report the presence of a new type of wind streak [5].

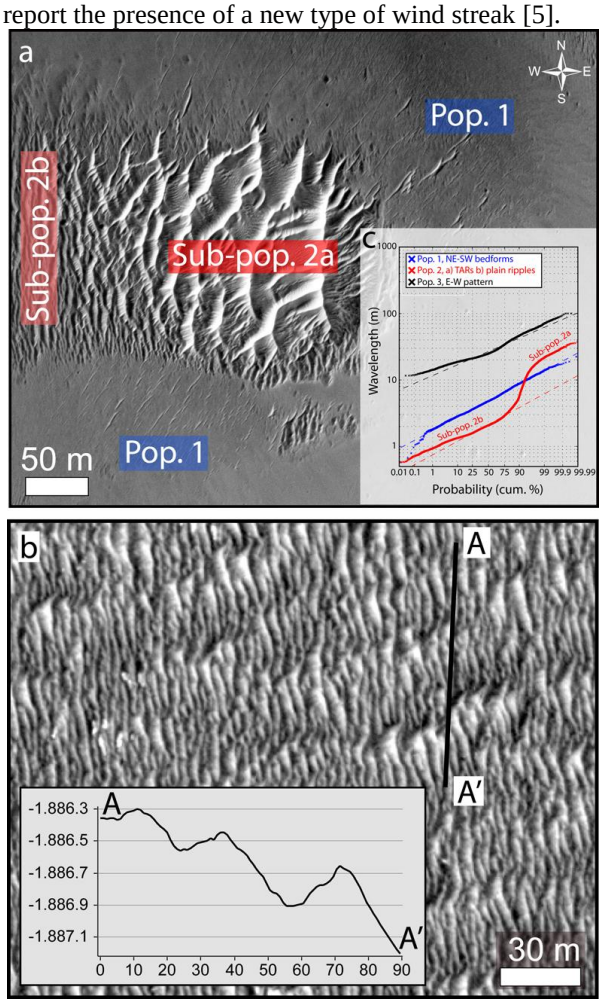

Fig. 1: a) Population 1 and 2. Pop. 2 can be divided into two supopulations 2a (intra-crater TARs) and 2b (plain ripples) **b)** Population 3 formed by E-W trending elevated ridges **c)** Log-normal probability plot for bedforms wavelength measurements.

Methods: Aeolian bedform have been mapped over ten HiRISE images [6] (data availability at the time of writing) that we coregistered over a regional 100 m/pixel THEMIS infrared mosaic. We mapped the aeolian bedforms in automatic and manually. We used the automatic approach to study one representative example of ripple streak using the method of [7]. Bedform wavelength has been extracted to statistically segregate the different populations visually identified on HiRISE [8]. In order to derive the present-day wind directions, we manually mapped the bright and dark wind streaks. Bedform height is computed on a digital terrain model (DTM) (spatial resolution=1 m/pixel) built using the NASA Ames Stereo Pipeline [9] from one HiRISE stereo couple on the SE landing ellipse.

Three bedform populations: We identified three morphologic populations (Figs. 1 and 2): Population 1, the most recent episode of aeolian construction, is confined inside craters and consists of NE-SW trending bedforms (formative winds from the NW or the SE assuming a transverse nature for these features) and superimpose the N-S trending bedforms of the population 2. The latter is represented by the emplacement of the plain ripples (sub-population 2b) and the accumulation of TARs inside impact craters (sub-population 2a) (Fig. 1a). The main N-S trend of the population 2 bedforms indicate dominant winds from the east. The 2b megaripples are grouped in bands defining an additional bedform orientation trending E-W, the population 3 (Fig. 1b) [10]. Wavelength differences in the 2b ripples mark the different bands which can be identified in digital terrain models as elevated ridges ~0.1-0.3 m in height (Fig. 1b). Wavelength lognormal plot distribution for the different populations visually identified indicate that the 3 bedform groups distinguished visually constitute distinct populations (Fig. 1c).

The population 3: This enigmatic group of features may represent: 1) the reworking of a relict E-W trending pattern (most likely TARs) subsequently reworked by the 2b plain ripples [10]; 2) or a longitudinal "ribbon pattern" [11,12]. Ribbons features represent a mode of self-organization that is still poorly understood, likely due to small scale rotatory flows caused by the change in the roughness at the flow/bed interface [13]. Thus ribbons occurrence seems to be related to strong uni-directional winds acting on bimodal sand bed. This would change our evolutionary scenario with

the population 3 pattern forming together with the population 2b under the influence of the same strong easterlies.

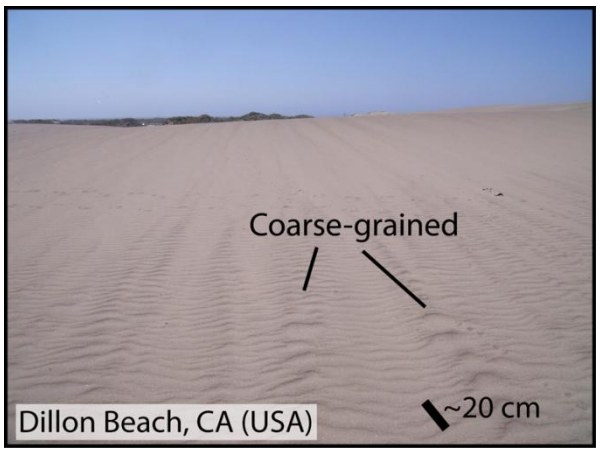

Fig. 2: Sand ribbons at Dillon Beach, CA, USA (photo taken by the author).

Ripple streaks: The ripple wavelength spatial distribution in the population 2 is strongly topographically controlled. The larger wavelength plain ripples (subpopulation 2b) tend to cluster in the wake zone of impact craters forming "megaripple tails" (ripple streaks) which extend downwind in a western direction (Fig. 3) [5]. Ripple streaks can be classified as a new type of wind streak for two reasons: they are not variable features as the streaks described in [14]. Unlike the dark depositional streaks [15] the ripple streaks do not source from an intra-crater deposit. The crater topography played a key role in generating local wind conditions favorable for bedform development, as showed in laboratory experiments [16,17,18]. The observed wavelength distribution can be related to the higher wind speed in the lee of the crater or can be the result of grain size segregation. These two factors can help to explain both E-W and N-S wavelength variations, but the relative contribution of each one can only be assessed by detailed *in situ* investigations. Their westward orientation give further hints on the regional easterlies that emplaced the population 2 bedforms.

Conclusion: Our results show that the study area has been subject to diverse winds that have generated a complex bedform pattern. With the exception of the population 1 pattern, the direction of the winds responsible for the emplacement of the aeolian features described in this work differ from the present day wind directions. Future measurements from the ExoMars 2016 DREAMS package, combined with Opportunity data can help to better decipher the nature of the population 3 and the wind regime in Meridiani Planum.

References: [1] Bettanini C. et al. (2014) *Proc. of IEEE Metrology for Aerospace* 448, pp. 167–173. [2] Sullivan R. et al. (2005) *Nature* 436. [3] Golombek M. et al. (2010) *JGR* 111. [4] Fenton L.K. et al. (2015) *Aeol. Res.* pp. 75-99. [5] Silvestro S. et al. (2014) *8th Int. Conf. on Mars* [6] McEwen et al. (2007) *JGR* 112. [7] Vaz D. A. and Silvestro S. (2014) *Icar*. 230, 151-161 [8] Ewing R. C. et al. (2006) *ESPL* 31. [9] Moratto et al. (2010) *41st LPSC*. [10] Silvestro et al. (2014) http://www.hou.usra.edu/meetings/8thmars2014/eposter/1193.pdf. [11] Allen J. R. L. (1968) North-Holland pub. Co. [12] Allen J. R. L. (1982) Elsevier Science. [13] Bagnold (1956) Dover Pub. INC. [14] Sagan et al. (1972) *Icar*. 372(17). [15] Thomas et al. (1981) *Icar*. 45, 124-153. [16] Tyler (1979) USGS Professional Paper n. 1052 pp. 171-185. [17] Greeley R. and Iversen J. (1985) Cambridge Univ. Press. [18] Vevereka J. et al. (1981) *Icar*. 45 154-166.

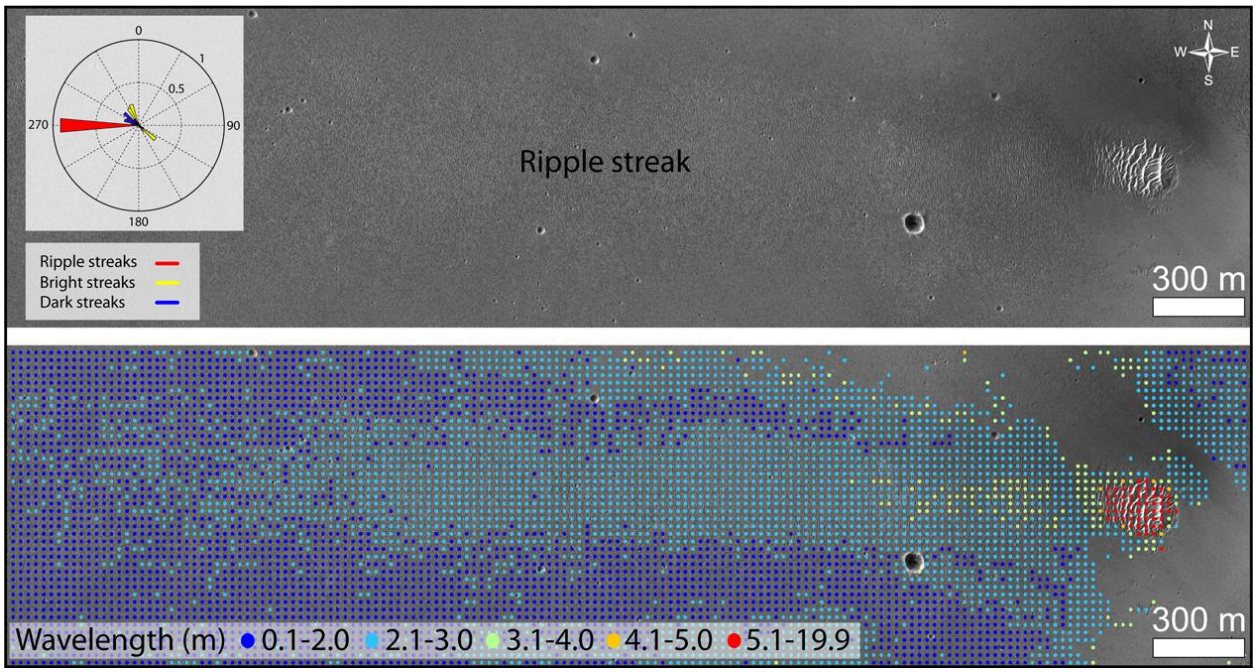

Fig. 3: Bedform wavelength spatial distribution along a typical ripple streak. Ripple and active wind streak orientations (rose diagram in inset).